Potential Mechanism of Guizhi Decoction in Hypertension Treatment Based on Network Pharmacology and Dahl Salt-Sensitive Rat Model

Ji-ye Chen
Shandong University of Traditional Chinese Medicine
Yong-jian Zhang
Shandong University of Traditional Chinese Medicine
Yong-cheng Wang
Affiliated Hospital of Shandong University of Traditional Chinese Medicine
Guo-feng Zhou
Shandong University of Traditional Chinese Medicine
Xiao Li (lixiao617@hotmail.com)
Affiliated Hospital of Shandong University of Traditional Chinese Medcine https://orcid.org/0000-0003-2656-5301

Research

Keywords: Guizhi decoction, Network pharmacology, Hypertension, Molecular docking, Molecular mechanism

Posted Date: September 22nd, 2020

DOI: https://doi.org/10.21203/rs.3.rs-76638/v1

Abstract

Background

Guizhi decoction (GZD), a classical Chinese herbal formula, has been widely used to treat hypertension, but its underlying mechanisms remain elusive. The present study aimed to explore its therapeutic effects and potential mechanisms in the treatment of hypertension using network pharmacology and experimental validation.

Methods

The active ingredients and corresponding targets were collected from Traditional Chinese Medicine Systems Pharmacology database and Analysis Platform (TCMSP). The targets related to hypertension were identified from multiple databases, and multiple networks were constructed to identify key compounds, hub targets, and main biological processes and pathways of GZD against hypertension. The Surflex-Dock software was used to validate the binding affinity between key targets and their corresponding active compounds. The Dahl salt-sensitive rat model was used to evaluate the therapeutic effects of GZD on hypertension.

Results

A total of 112 active ingredients, 222 targets of GZD and 341 hypertension- related targets were obtained. Furthermore, 56 overlapping targets were identified, five of which were determined as the hub targets to perform experimental verification, including interleukin 6 (IL-6), C-C motif chemokine 2 (CCL2), IL-1β, matrix metalloproteinase 2(MMP-2), and MMP9. Pathway enrichment

Introduction

Hypertension is one of the most common cardiovascular diseases worldwide.[1] Although substantial progress has been made in recent years in the diagnosis and therapy of hypertension, it remains one of the most severe public health issues in the world. It is predicted that more than 1.5 billion people worldwide will suffer from hypertension by 2025, and this situation is expected to worsen over the next decade with the increasing global and ageing populations[2, 3]. Furthermore, long-lasting hypertension usually leads to myocardial infarction, stroke, chronic kidney dysfunction, heart failure, and other complications, which are the major causes of disability and premature death in humans.[4] Generally, the pathological mechanisms of hypertension are mainly related to the overactivation of the renin-angiotensin-aldosterone system (RAAS) and sympathetic nervous system (SNS), and sodium and water retention.[2, 4] Hence, the first-line medications for hypertension treatment primarily include diuretics, β-blockers, calcium channel blockers, angiotensin-converting enzyme inhibitors, and angiotensin II receptor blockers.[5] However, some antihypertensive medications are reportedly associated with numerous side

effects including peripheral edema, anemia, persistent cough, and decreased sexual function.[2, 4, 5] Therefore, it is necessary to develop more feasible and safer therapeutic strategies for the management of hypertension.

Cumulative valuable research showed that Chinese medicinal formulas, such as Xiao Yao San, Banxia Baizhu Tianma decoction, and Niuhuang Jiangya preparation, demonstrated satisfactory efficacy and minimal side effects in the treatment of hypertension.[6–8] Therefore, several scholars are paying attention to the scientific research value of traditional Chinese medicine (TCM) in the prevention and management of hypertension.[6] According to the TCM therapeutic theory of "regulating Ying-Wei in case of heart damage," we have discovered an association between the dysfunction of Ying-Wei and hypertension-related clinical symptoms. Guizhi decoction (GZD) is a classical TCM prescription for the treatment of Ying-Wei disharmony.[9] GZD is composed of five Chinese medicinal herbs: *Cinnamomi ramulus* (Guizhi, GZ), *Paeoniae radix alba* (Baishao, BS), *licorice* (Gancao, GC), *Zingiber officinale roscoe* (Shengjiang, SJ), and *Jujubae fructus* (Dazao, DZ). Our previous study showed that GZD not only effectively reduced blood pressure, but also prevented myocardial fibrosis, restored balance in the autonomic nervous system, and inhibited the expression of pro-inflammatory cytokines in the Dahl salt-sensitive rats.[10] Additionally, we found that GZD could significantly improve the heart rate variability and the activity of the vagus nerve associated with the progression of hypertension.[9] However, the underlying mechanisms and targets of GZD against hypertension are not fully understood, which have impeded its clinical practice. Further research should be conducted to provide scientific evidences regarding the clinical usage of GZD in hypertension treatment.

TCM prescriptions are a complicated system that usually interact with multiple targets and multiple channels to exert their pharmacological effects; hence, it is relatively difficult to elucidate their active ingredients and therapeutic mechanisms.[11] Network pharmacology is an innovative approach based on computational systems pharmacology that can accurately decipher the association among the drugs, targets, and diseases at a systematic and comprehensive level.[12] The systematic and holistic characteristics of network pharmacology correspond to the concepts of holistic view and dialectical treatment theory of TCM, providing a scientific basis for the in-depth study of TCM prescriptions.[13] Currently, there is growing evidence about the reliability of the network pharmacology method, which may be an effective way to study the pharmacological mechanisms of TCM prescriptions.[11–14]

In this study, network pharmacology analysis was used to visualize and decipher the complex relationships among the key compounds, targets, main biological processes and pathways, and disease. Moreover, molecular docking experiment was used to validate the binding affinity between key targets and their corresponding active compounds. Finally, the therapeutic effect of GZD on hypertension was validated by an experimental model. The detailed flowchart is illustrated in Fig. 1.

Methods

Identification of active compounds and prediction of corresponding targets of Guizhi decoction

The active constituents of the five herbal medicines in GZD were acquired from the Traditional Chinese Medicine Systems Pharmacology database and Analysis Platform (TCMSP) (http://lsp.nwu.edu.cn/tcmsp.php). This database provides comprehensive and accurate compound information, including the herbal ingredients' chemical structural data, drug half-life, oral bioavailability (OB), intestinal epithelial permeability, and drug-likeness (DL).[15] According to the recommended drug screening criteria of the TCMSP database, chemical constituents with OB ≥ 30% and DL ≥ 0.18 may present ideal pharmacological activities, and they were selected as the active ingredients for further analysis. Subsequently, we screened the targets of active ingredients in GZD through the TCMSP database. The target names were imported into the UniProt database (http:// www.uniprot.org/) with the species selected as "Homo sapiens," and the gene names of the targets were obtained from the UniProt database.

Identification of hypertension-related targets

"Hypertension" was the keyword used to extract the hypertension-related targets from the Online Mendelian Inheritance in Man (OMIM, https://omim.org/), Comparative Toxicogenomics Database (CTD, http://ctdbase.org/), Genecards (http://www.genecards.org/), and Drugbank (https://www.drugbank.ca/) databases. The disease-related targets obtained were standardized as gene names from the UniProt database with the species selected as "Homo sapiens." A Venn diagram was drawn using an online website (http://bioinformatics.psb.ugent.be/Webtools/Venn/) to obtain the overlapping targets between the hypertension-related targets and active compound-related targets, which could be the potential targets of GZD in hypertension treatment.

Construction of protein-protein interaction network and screening of hub targets

The Search Tool for the Retrieval of Interacting Genes (STRING) database (https://string-db.org/) can explore and analyze direct and indirect interactions between proteins.[16] Based on the overlapping targets of GZD and hypertension, we constructed the protein-protein interaction (PPI) network by using the STRING 11.0 database with the species limited to "Homo sapiens" and confidence score > 0.7. The degree value was applied to choose the putative targets for molecular docking and experimental verification.

Gene ontology and pathway enrichment analyses

For better clarification of the potential biological processes and pathways of GZD in the treatment of hypertension in this study, we utilized the Database for Annotation Visualization and Integrated Discovery (DAVID, https://david.ncifcrf.gov/) to conduct gene ontology (GO) function enrichment analysis and the Kyoto Encyclopedia of Genes and Genomes (KEGG) pathway enrichment analysis. The GO terms and pathway terms with p-value ≤ 0.05 were considered significant enrichment entries.

Network construction and analysis

In this study, several networks were established to visualize and analyze the complicated interconnection of compounds, targets, and disease using Cytoscape 3.7.1 software (https://cytoscape.org/; version 3.7.1). Based on the results, the compound-target (C-T) network, target-disease (T-D) network, compound-target-disease (C-T-D) network, and target-pathway (T-P) network were constructed using Cytoscape software. In these networks, nodes of different colors and shapes represented different active compounds, potential targets, or signal pathways, and the edges represented the connections between the nodes.

Molecular docking.

The Surflex-Dock program in SYBYL 2.1 software (Certara Inc., USA) was applied to verify the network pharmacology screening results by docking the key targets with their active compounds and positive anti-hypertension drugs. The Surflex-Dock program is one of the most efficient ligand-receptor docking techniques and virtual screening programs with favorable features of high precision, high true-positive rate, and fast speed.[17] Common antihypertensive agents, valsartan, candesartan, captopril, enalapril, furosemide, metoprolol, nifedipine, amlodipine, bisoprolol, and hydrochlorothiazide were used as positive drugs for molecular docking. Seventeen key targets with degrees > 30 in the PPI network were selected for docking simulation, and these targets were mapped to 80 active compounds for molecular docking. The three-dimensional structures of the active compounds were downloaded from the PubChem database (https://pubchem.ncbi.nlm. nih.gov/). The structures of the key target proteins were downloaded from the Protein Data Bank database (http://www.pdb. org/) and modified through the Surflex-Dock software.[18] The complex ligand and water molecules in protein receptors were removed, hydrogen atoms were added to the receptor, and amino acids were optimized and patched.[19] After molecular docking with the default parameters, the docking score values were generated for each compound docking with key targets. The docking score could be used to estimate the binding capacity between the targets and their active compounds.

Experimental animals and protocol

Six-week-old male, specific pathogen-free (SPF) grade Dahl salt-sensitive rats (body weight, 160–180 g) were provided by the Charles River Animal Laboratory (Beijing, China, Certificate No. 2016-0006). The rats were reared in the SPF room at a temperature of 20 ± 2℃ and 50 ± 10% humidity on a 12 h light/dark cycle. After acclimatization for 1 week, systolic blood pressure of all rats was measured weekly using a 12-channel tail-cuff blood pressure system (MRBP, IITC Life Science Instruments, USA). All experimental protocols used in this study were performed in accordance with the Institutional Animal Care and Use Committee of Shandong University of Traditional Chinese Medicine (Permit Number: SDVTCM2018071501).

Preparation of Guizhi decoction and intervention

The herbal medicines were supplied by the Affiliated Hospital of Shandong University of Traditional Chinese Medicine (Jinan, China) and verified by Prof. Feng Li. *Cinnamomi ramulus*, *Paeoniae radix alba*, and *licorice* were mixed in the standard ratio of 3:2:2, with reflux extraction of 10 times the volume of distilled water twice for 1 h each. The extracts were then mixed thoroughly, and concentrated to a relative density of 1.20–1.25 (70–80°C). The solution with 1.5 g/mL of the initial herb was applied in further experiments. After 1 week of acclimatization, the rats were randomly allocated to three groups (n = 8, each): NS group (normal-salt diet), HS group (high-salt diet), and GZD group. The NS group was fed low-salt (0.3% NaCl) diet throughout the experimental period. At 8 weeks of age, the HS group and GZD group fed with high-salt (8% NaCl) diet progressively developed hypertension. At 12 weeks of age, the NS and HS groups were fed with physiological saline at 2 mL/day, while 2 mL/4.0 g of GZD crude drug/kg/day was administered to the GZD group according to the results of a previous study.[9]

Collection of left ventricle tissue

At the end of the experiment, all the rats were anesthetized by intraperitoneal injection of 20 mg/kg pentobarbital sodium. The left ventricle of each rat was carefully isolated and cut into three parts. One part was fixed in 6% paraformaldehyde solution for morphological examination. The second part was fixed in 2.5% glutaraldehyde solution and observed under transmission electron microscope. The last part was placed in liquid nitrogen for western blot and quantitative real-time polymerase chain reaction (qRT-PCR).

Histological examination and transmission electron microscopy

The left ventricles were cut into 4-μm sized sections, and they were subjected to hematoxylin-eosin (H&E) staining or Masson staining to evaluate inflammatory cell infiltration or cardiac fibrosis, respectively.[10] Histological images of myocardium in rats were detected using ZEN 1.01.0 Imaging analysis software (Carl Zeiss Microscopy GmbH, German). Additionally, transmission electron microscopy was used to reveal the extent of myocardial damage.

Quantitative real-time polymerase chain reaction

In order to verify the reliability of network pharmacology analysis, qRT-PCR experiments were used to examine the mRNA expression levels of hub targets in the PPI network. Total RNA of the left ventricle was isolated using Trizol (Invitrogen, USA), and reverse transcription was performed with the PrimeScript RT reagent kit with gDNA Eraser (Takara, Japan) for 5 min at 85°C according to the manufacturer's instructions. The Light Cycler 480 SYBR Premix Ex Taq II (Roche, Germany) was used to perform qRT-PCR. The reaction conditions were 94°C for 2 min, 94°C for 30 s, and 60°C for 30 s, and 40 cycles were performed in total. Each RNA sample was performed in triplicate, and the results were normalized with β-actin. The relative quantification analysis was performed by the $2^{-\Delta\Delta CT}$ method.

The sequences of the primers (synthesized by Accurate Biotechnology Co., Ltd) were designed as follows: IL-6: 5'-ATTGTATGAACAGCGATGATGCAC-3'/5'-CCAGGTAGAAACGGAACTCCAGA-3'; IL-1β: 5'-

CCCTGAACTCAACTGTGAAATAGCA-3'/5'-CCCAAGTCAAGGGCTTGGAA-3'; CCL2: 5'-CTATGCAGGTCTCTGTCACGCTTC-3'/5'-CAGCCGACTCATTGGGATCA-3'; MMP-2: 5'-ACCTTGACCAGAACACCATCGAG-3'/5'-CAGGGTCCAGGTCAGGTGTGTA-3'; MMP-9: 5'-AGCCGGGAACGTATCTGGA-3'/5'-TGGAAACTCACACGCCAGAAG-3'; and β-actin: 5'-GGAGATTACTGCCCTGGCTCCTA-3'/5'-GACTCATCGTACTCCTGCTTGCTG-3'.

Western blot analysis

Western blot experiment was performed to assess the protein expression levels of the hub targets in the PPI network. The left ventricles were lysed by adding radioimmunoprecipitation assay lysis (RIPA) buffer (Cat. No. P0013B, Beyotime Biotechnology) and phenylmethylsulfonyl fluoride (PMSF, Cat. No. ST506, Beyotime Biotechnology). The protein concentration was measured using the bicinchoninic acid assay kit (Cat. No. P0010, Beyotime Biotechnology). Equal amounts of protein lysates were separated via appropriate concentration of sodium dodecyl sulfate-polyacrylamide gel electrophoresis (Cat. No. P0012A, Beyotime Biotechnology). The proteins were then transferred to the polyvinylidene difluoride membrane and cultured in 5% non-fat dry milk in Tris buffered saline-Tween 20 (TBST) buffer for 60 min at room temperature. Subsequently, the membranes were incubated with the CCL2 (Cat. No. ab25124, Abcam, 1:2000), IL-6 (Cat. No. ab9324, Abcam, 1:1000), IL-1β (Cat. No. ab205924, Abcam, 1:1000), MMP-2 (Cat. No. 10373-2-AP, Proteintech, 1:1000), MMP-9 (Cat. No. 10375-2-AP, Proteintech, 1:1000), and β-actin (Cat. No. ab8226, Abcam, 1:5000) overnight at 4°C. The membranes were rinsed five times in TBST, and then incubated with secondary antibodies for 1 h at room temperature. The protein bands were infiltrated with enhanced chemiluminescence, and they were visualized using the FluorChem Q 3.4 system (ProteinSimple, USA).

Statistical analysis

Data were expressed as mean ± standard deviation. The differences between groups were analyzed by one-way analysis of variance and independent t-tests using Statistical Package for the Social Sciences 21.0 software (SPSS, USA). A p-value < 0.05 was considered statistically significant.

Results

Screening of the active compounds and targets prediction

A total of 146 active ingredients of five herbal medicines in GZD were identified based on threshold values of OB ≥ 30% and DL ≥ 0.18, including 7 compounds in GZ, 13 compounds in BS, 92 compounds in GC, 5 compounds in SJ, and 29 compounds in DZ. After deleting the duplicate data, 112 active ingredients were selected for further analysis. The detailed informations of active ingredients are listed in Supplementary file, Table S1. Moreover, 222 targets of active compounds of GZD were obtained from the TCMSP database and the gene names of these targets were collected via the Uniprot database (Supplementary file, Table S2).

Compound-target network construction and analysis

In order to reflect the interactions intuitively between the active compounds of GZD and their potential targets from a systematic and holistic view, the C-T network was constructed by mapping 112 active compounds to their 222 corresponding potential targets. As shown in Fig. 2a, the network consisted of 339 nodes (5 herbal medicines nodes, 112 active compound nodes, and 222 compound-associated target nodes) and 1932 interaction edges. In the network, quercetin (degree 272), β-sitosterol (degree 104), and kaempferol (degree 102) showed the maximum interactions with potential targets, indicating that these active compounds with high degree values could play an important role in the potential pharmacological effects of GZD. The C-T network showed intimate communications between active compounds and related targets, which provided reference to investigate the pharmacological mechanisms of GZD further.

Screening of hypertension-related targets and construction of disease-target network

A total of 477 targets associated with hypertension were identified from the CTD, GeneCards, OMIM, and Drugbank databases. We chose the top 200 results related to hypertension with the highest relevance from GeneCards as major targets of hypertension. After duplicate targets were deleted, 341 hypertension-related targets were finally obtained. These targets were then uploaded to Cytoscape 3.7.1 for visualization. The D-T network consisted of 342 nodes (1 hypertension node and 341 hypertension-target nodes) and 477 edges. Figure 2b shows the top 14 targets with the highest degree values (degree ≥ 100) were recognized as the most crucial targets in the D-T network, namely INS, ALB, AKT1, IL-6, VEGFA, TNF, NOS3, REN, EDN1, AGT, TP53, ACE, FN1, and IGF1. Therefore, these targets could be the potential targets for the treatment of hypertension.

Construction of PPI network

PPI network was established to better interpret the mechanisms of GZD in hypertension treatment by using STRING software. As shown in Fig. 2c, we obtained 56 overlapping targets after merging hypertension-related targets and active compound-related targets. A PPI network was then established by importing the overlapping targets to the STRING database. As shown in Fig. 2d, the network consisted of 56 nodes and 627 edges with an average node degree of 22.40, network centralization of 0.464, and an average number of neighbors of 22.393. Based on the degree principle of each target, IL-6, CCL2, IL-1β, MMP-9, and MMP-2 were determined as the hub targets to perform experimental verification.

Construction of compound-target-disease network

In order to illustrate the complex relationship among the active compounds, overlapping targets, and hypertension, we constructed the C-T-D network. The network comprised of 165 nodes (107 active compounds, 56 potential targets, 1 formula, and 1 disease) and 762 edges. In this network, the key active compounds of GZD against hypertension mainly included quercetin (degree = 84), kaempferol (degree = 40), and β-sitosterol (degree = 24), which exhibited degree values higher than that of other compounds. As shown in Fig. 3, the same target could interact with different active compounds, and the same compound

could act on multiple targets. These results suggested that GZD exhibits multi-component and multi-target characteristics in the treatment of hypertension.

Gene ontology enrichment analysis and target-pathway network construction

To reveal the functional role of the 56 overlapping targets further, GO functional analyses were conducted in the DAVID database. The results of GO enrichment analysis included 254 biological processes (BP), 27 cell components (CC), and 35 molecular functions (MF) with a threshold value of $p \leq 0.05$. The top 10 GO analysis results listed in each term are shown in Fig. 4a-c. The BP results mainly comprised of response to hypoxia, response to drug, aging, inflammatory response, and angiogenesis. The CC analysis indicated that the overlapping targets were mainly related to extracellular space, caveola, membrane raft, extracellular region, and plasma membrane. The MF results mainly included protein binding, protein homodimerization activity, protein heterodimerization activity, enzyme binding, and transcription factor binding.

The results of the KEGG enrichment analysis showed that 63 pathways meeting the threshold value of $p < 0.05$ were considered as significant enrichment pathways. After sorting according to the p-value, the top 20 pathways and overlapping targets were used to construct the T-P network using Cytoscape 3.7.1 software. As depicted in Fig. 4d, the KEGG pathways of GZD against hypertension were mainly related to the tumor necrosis factor (TNF) signaling pathway, hypoxia-inducible factor 1 (HIF-1) signaling pathway, toll-like receptor (TLR) signaling pathway, insulin resistance, PI3K-AKT signaling pathway, and nuclear factor kappa-B (NF-κB) signaling pathway.

Docking results analysis

The docking scores of the 17 key targets are shown in Fig. 5, ranging from 0 to 10, and representing the binding ability from weak to strong. The docking scores and the spatial structure showed that multiple active compounds of GZD show tight binding ability with the key targets, which further indicates that the specific therapeutic effect of GZD in the treatment of hypertension, especially for β-sitosterol, kaempferol, and quercetin, were very close to the Vina scores of furosemide and nifedipine. As shown in Fig. 6, we observed that many active compounds could form hydrogen bonds with the key targets.

Effect of Guizhi decoction on the blood pressure in rats

As shown in Fig. 7, no obvious differences were observed in the systolic blood pressure between the HS group and GZD group before administration of GZD. The systolic blood pressure in these two groups was significantly higher than that of the NS group at 8 weeks of age ($p < 0.01$). After 4 weeks of GZD administration, systolic blood pressure in the GZD group reduced as compared to the HS group ($p < 0.01$).

Effect of Guizhi decoction on inflammation in rats

As presented in Fig. 8a, H&E staining showed that the ratio of inflammatory cell infiltration in the HS group was remarkably higher than that of the NS group ($p < 0.01$), but this pathological change markedly reduced after administration of GZD ($p < 0.01$). As shown in Figs. 8b and 9, the mRNA and protein expressions of IL-6, CCL2, and IL-1β were significantly higher in the HS group than in the NS group ($p < 0.01$). After administration of GZD for 4 weeks, the mRNA and protein expressions of IL-6, CCL2, and IL-1β were obviously lowered as compared to the HS group ($p < 0.01$).

Effect of Guizhi decoction on the myocardial fibrosis in rats

In the results of transmission electron microscopy, the HS group presented disordered arrangement of the cardiomyocytes, apparent myocardial injury, and excessive collagen fibers, which were markedly attenuated with GZD treatment (Fig. 10a). Similarly, the results of Masson staining showed that the degree of interstitial fibrosis decreased in the GZD group as compared to the HS group (Fig. 10b, $p < 0.01$). As shown in Figs. 9 and 10c, the mRNA and protein expressions of MMP-2 and MMP-9 were significantly higher in the HS group as compared to the NS group ($p < 0.01$). After 4 weeks of GZD treatment, the mRNA and protein expression of MMP-2 and MMP-9 in the GZD group were obviously decreased as compared to the HS group ($p < 0.05$ and $p < 0.01$, respectively), suggesting that GZD could decrease mRNA and protein expression of MMP-2 and MMP-9 to improve the collagen deposition in Dahl salt-sensitive rats.

Discussion

Hypertension is a multifactorial disease affected by the complex interactions between genetic predisposition and environmental factors.[4] There have been several successful experiences in the treatment of cardiovascular diseases such as hypertension with GZD.[9, 10, 20] However, its material basis and potential mechanism have not been fully elucidated. In the present study, we initially identified key compounds, hub targets, and main biological processes and pathways of GZD against hypertension by network pharmacology analysis, and then examined the therapeutic effects of GZD on hypertension in the Dahl salt-sensitive rat model. Our integrative approach uncovered the potential mechanisms of GZD against hypertension from the systematic network perspective and demonstrated that GZD can effectively attenuate elevated blood pressure, improve both inflammatory cell infiltration and myocardial fibrosis, and inhibit the expression levels of IL-6, CCL2, IL-1β, MMP-2, and MMP-9 in the Dahl salt-sensitive rats.

In this study, 112 active compounds of GZD were identified from the TCMSP database, and we screened out three key compounds by the network analysis that might have potential anti-hypertensive function. The three key active compounds were β-sitosterol, kaempferol, and quercetin. Moreover, these three key compounds exhibited optimal binding affinity in molecular docking, indicating that they might play a crucial role in the anti-hypertensive effects of GZD. β-sitosterol is a type of phytosterol that exerts protective cardiovascular effects mainly by increasing the intracellular antioxidant defense, improving endothelial function, and inhibiting serum cholesterol levels.[21–23] Kaempferol has shown to be

effective in maintaining blood pressure by effectively repressing the generation of inflammatory cytokines and apoptosis, stimulating the release of NO from the vascular endothelium, and decreasing myocardial fibrosis by inhibiting proliferation of cardiac fibroblasts.[24–26] Quercetin exerts remarkable effects in the treatment of hypertension by improving the endothelial function by increasing NO bioavailability and NO production, inhibiting the overactivation of RAAS, and reducing the generation of the adhesion molecules and other inflammatory factors.[27, 28] Overall, these observations suggest that the key compounds of GZD could be crucial in the treatment of hypertension.

In the PPI network, we observed that IL-6, CCL2, IL-1β, MMP-2, and MMP-9 were the hub targets of the GZD for improving hypertension. Notably, these hub targets were closely related to various compounds and biological processes and pathways based on the analysis of multi-layered networks, suggesting that these targets may be important in the role of GZD against hypertension. Several studies showed that a long-term inflammatory response can trigger the sympathetic activation and result in myocardial fibrosis and endothelial dysfunction.[29] Thus, the inhibition of inflammatory response can effectively delay or control the development of hypertension and severe complications.[30] The inflammatory process of hypertension is characterized by increased levels of local inflammatory cytokines such as IL-6, IL-1β, TNF-α, and ICAM-1, which are highly correlated with increased risk of hypertension, and they could be useful diagnostic tools for hypertension in the future.[4] Particularly, IL-6, a well-known pro-inflammatory cytokine, participates in the pathological process of hypertension by promoting endothelial dysfunction and inflammatory cell recruitment.[31] The inhibition of IL-1β could inhibit the overactivation of RAAS and decrease overproduction of other pro-inflammatory cytokines, thereby improving hypertension and cardiac fibrosis.[32, 33] CCL2 is a chemokine that contributes to progression of hypertension by recruiting the circulating monocytes to the blood vessel walls and promoting macrophage infiltration.[34] Myocardial fibrosis is a crucial pathological feature in the progression of hypertension, and it is predominantly related to an excessive accumulation of extracellular matrix proteins that contribute to increased ventricular wall stiffness and impaired diastolic function.[32, 35] MMPs participate in the development of myocardial fibrosis by regulating the degradation and production of collagen, and higher levels of MMP-2 and MMP-9 were considered as markers of cardiovascular risk and aberrant accumulation of collagen.[36, 37] As expected, our experimental results showed that GZD can reduce the degree of inflammatory infiltration and area of interstitial fibrosis, as well as downregulate the protein and mRNA levels of IL-6, IL-1β, CCL2, MMP-9, and MMP-2 in Dahl salt-sensitive rats. These results were in line with earlier reports that showed that the improvement of cardiac inflammation and fibrosis was associated with decrease in blood pressure.[10, 38]

Based on the results of the network analysis and molecular docking, several targets such as AKT1, VEGFA, eNOS, ICAM-1, PTGS2, and ALB could be associated with the potential effect of GZD on hypertension. For example, AKT1 directly participates in the phosphorylation of eNOS at serine 1177, which could increase enzyme activity, NO production, and angiogenesis.[39] Vascular endothelium is implicated in the regulation of vascular tone and structure, and the abnormal vascular endothelial function could be a major contributor to the adverse outcomes of hypertension.[4, 40] VEGFA serves as a homologue of the VEGF family and regulates cell migration, division, and angiogenesis regulation in

normal microvascular endothelial cells.[41] Several studies have provided evidence that eNOS is a significant contributor in the maintenance of vascular function and cardiovascular homeostasis.[42] NO, produced by eNOS, mediates control of the inflammatory process as well as regulation of neoangiogenesis and vasodilatation. The decrease in bioavailability of NO has been implicated as a major cause of endothelial dysfunction in hypertension.[4] ICAM-1 promotes the adhesion of leukocytes and vascular endothelial cells, and subsequently leukocyte activation, which probably triggers the endothelial dysfunction, inflammatory response, and blood-vessel remodeling.[32, 43] PTGS2-derived products have been proven to be extensively linked with the regulation of fluid balance, endothelial function, and ROS production.[44]As a major protein in human serum, the low level of serum ALB is associated with hypertension, increased risk of cardiovascular disease, and carotid atherosclerosis.[45] These targets need to be verified in follow-up experiments.

In the KEGG pathway analysis, the overlapping targets were related to multiple pathways, such as TNF signaling pathway, HIF-1 signaling pathway, TLR signaling pathway, insulin resistance, PI3K-AKT signaling pathway, and NF-κB signaling pathway. These signaling pathways play a significant role in the pathogenesis and management of hypertension. The activation of the TNF signaling pathway is an important contributor to inflammatory processes, which plays an essential part in modulating the gene expression of many cytokines and chemokines involved in vascular inflammation and remodeling.[46] In the inflammatory process associated with hypertension, the inappropriate activation of the NF-kB pathway facilitates disease progression by inducing inflammatory cytokine release, vascular dysfunction, and generation of reactive oxygen species.[32, 47] The TLR signaling pathway, a critical upstream mechanism activating inflammatory signaling, regulates the inflammatory response by directly promoting the release of a variety of inflammatory mediators, inducing the migration of immune cells to inflammatory sites, and increasing the adhesion and infiltration ability of inflammatory cells.[29, 48] The HIF-1 pathway is highly correlated with energy metabolism and angiogenesis, and participates in the pathophysiology of inflammation and ischemia. HIF-1 is the chief hypoxia-regulated transcription factor that regulates cellular responses in hypoxic and ischemic conditions.[49, 50] The PI3K/AKT pathway plays a seminal role in regulating multiple biological effects, including cell growth and proliferation, apoptosis, and angiogenesis.[51] The PI3K/AKT pathway could activate the phosphorylation and activation of eNOS, and maintain blood pressure homeostasis, endothelium function, and vascular integrity.[52] Insulin resistance is a risk factor in hypertensive patients that closely correlates with the activation of RAAS and SNS, resulting in increased peripheral vascular resistance and circulating plasma volume.[53] Therefore, the improvement of insulin resistance would be significant in the management of hypertension and its complications.[54] However, the effects of these signaling pathways in the mechanisms of GZD against hypertension need to be validated through rigorous investigations.

Because of the limitations regarding screening conditions of database and statistical software, several ingredients and targets of GZD against hypertension may have been missed during the screening process. Despite the limitations of this study, our results revealed the potential mechanism of GZD against hypertension, and provided scientific basis and valuable enlightenment for guiding future in-depth research and clinical applications.

Conclusion

In this study, the results of network pharmacology indicated that quercetin, β-sitosterol, kaempferol, and other effective compounds of GZD showed therapeutic efficacy in hypertension treatment by means of multiple targets and multi-pathways. Furthermore, the experimental results suggested that GZD could downregulate the expression levels of IL-6, IL-1β, CCL2, MMP-2, and MMP-9, thus inhibiting the inflammatory response and myocardial fibrosis in Dahl salt-sensitive rats. In conclusion, this study holistically illuminated the potential mechanisms of GZD in improving hypertension, and provided scientific basis for further pharmacological study and clinical applications.

Abbreviations

TCM: Traditional Chinese Medicine; TCMSP: Traditional Chinese Medicine Systems Pharmacology; DL: Drug-Like; OB: Oral Bioavailability; OMIM: Online Mendelian Inheritance; CTD: Comparative Toxicogenomics Database; PPI: Protein–Protein Interaction; DAVID: Annotation, Visualization and Integrated Discovery; GO: Gene ontology; BP: Biological process; KEGG: Kyoto Encyclopedia of Genes and Genomes; PTGS2: Prostaglandin- endoperoxide Synthase 2; INS:Insulin; REN:renin; EDN1: Endothelin-1; AGT:Angiotensin; TP53: Cellular tumor antigen p53; ACE:Angiotensin-converting enzyme; FN1:Fibronectin; IGF1:Insulin-like growth factor I; VCAM-Vascular cell adhesion protein; ICAM-Intercellular adhesion molecule; IL-6:interleukin-6; IL-1B:interleukin-1β; TNF-tumor necrosis factor; MMP-matrix metalloproteinase; IL-interleukin; NO-nitric oxide; eNOS-endothelial nitric oxide synthase; PI3K-phosphoinositide 3-kinase; AKT-serine/threonine-protein kinase; ALB-albumin; CCL2-C-C motif chemokine 2; VEGFA-Vascular endothelial growth factor A; NF-κB:Nuclear factor kappa-B; HIF-Hypoxia-inducible factor; TLR:Toll-like receptor.

Declarations

Disclosure

Ji-ye Chen, Yong-jian Zhang and Yong-cheng Wang are co-first authors of the article.

Availability of data and materials

The data used to support the findings of this study are available from the corresponding author upon request, unless there are legal or ethical reasons for not doing so.

Ethics approval and consent to participate

Not applicable.

Consent for publication

Not applicable.

Competing interests

The authors declare that they have no competing interests.

Funding

This research was supported by the National Natural Science Foundation of China (NO.81673970, 81874449 and 81804036).

Authors' Contributions

Xiao Li conceived and designed the experiments. Ji-Ye Chen, Yong-jian Zhang and Yong-cheng Wang wrote the manuscript together, contributed equally to this work, and are the co-first authors. Guo-feng Zhou collected and analyzed the data. All authors participated in the analysis and interpretation of the data and passed the final paper.

Acknowledgements

The authors would like to thank Dan Zhang and Yuan Li (Experimental Center of Shandong University of Traditional Chinese Medicine) for the technical support in the experiment.

References

1. James PA, Oparil S, Carter BL, et al. 2014 evidence-based guideline for the management of high blood pressure in adults: report from the panel members appointed to the Eighth Joint National Committee (JNC 8). Jama. 2014;311(5):507–20.
2. Olsen MH, Angell SY, Asma S, et al. A call to action and a lifecourse strategy to address the global burden of raised blood pressure on current and future generations: the Lancet Commission on hypertension. Lancet. 2016;388(10060):2665–712.
3. Kearney PM, Whelton M, Reynolds K, Muntner P, Whelton PK, He J. Global burden of hypertension: analysis of worldwide data. Lancet. 2005;365(9455):217–23.
4. Oparil S, Acelajado MC, Bakris GL, et al. Hypertension Nat Rev Dis Primers. 2018;4:18014.
5. Williams B, Mancia G, Spiering W, et al. 2018 ESC/ESH Guidelines for the management of arterial hypertension. Eur Heart J. 2018;39(33):3021–104.
6. Xiong X, Yang X, Liu Y, Zhang Y, Wang P, Wang J. Chinese herbal formulas for treating hypertension in traditional Chinese medicine: perspective of modern science. Hypertens Res. 2013;36(7):570–9.

7. Xiong X, Wang P, Duan L, et al. Efficacy and safety of Chinese herbal medicine Xiao Yao San in hypertension: A systematic review and meta-analysis. Phytomedicine. 2019;61:152849.
8. Wang H, Liu C, Zhai J, Shang H. Niuhuang Jiangya Preparation (a traditional Chinese patent medicine) for essential hypertension: A systematic review. Complement Ther Med. 2017;31:90–9.
9. Li X, Jiang YH, Jiang P, Yang JL, Ma DF, Yang CH. Effect of Guizhi Decoction ([symbols; see text]) on heart rate variability and regulation of cardiac autonomic nervous imbalance in diabetes mellitus rats. Chin J Integr Med. 2014;20(7):524–33.
10. Wang YC, Ma DF, Jiang P, et al. Guizhi Decoction Inhibits Cholinergic Transdifferentiation by Regulating Imbalance of NGF and LIF in Salt-Sensitive Hypertensive Heart Failure Rats. Chin J Integr Med. 2020;26(3):188–96.
11. Zhou Z, Chen B, Chen S, et al. Applications of Network Pharmacology in Traditional Chinese Medicine Research. Evid Based Complement Alternat Med. 2020, 2020:1646905.
12. Hopkins AL. Network pharmacology: the next paradigm in drug discovery. Nat Chem Biol. 2008;4(11):682–90.
13. Jian GH, Su BZ, Zhou WJ, Xiong H. Application of network pharmacology and molecular docking to elucidate the potential mechanism of Eucommia ulmoides-Radix Achyranthis Bidentatae against osteoarthritis. BioData Min. 2020;13:12.
14. Hu Q, Wei S, Wen J, et al. Network pharmacology reveals the multiple mechanisms of Xiaochaihu decoction in the treatment of non-alcoholic fatty liver disease. BioData Min. 2020;13:11.
15. Ru J, Li P, Wang J, et al. TCMSP: a database of systems pharmacology for drug discovery from herbal medicines. J Cheminform. 2014;6:13.
16. Szklarczyk D, Morris JH, Cook H, et al. The STRING database in 2017: quality-controlled protein-protein association networks, made broadly accessible. Nucleic Acids Res. 2017;45(D1):D362-d368.
17. Spitzer R, Jain AN. Surflex-Dock: Docking benchmarks and real-world application. J Comput Aided Mol Des. 2012;26(6):687–99.
18. Burley SK, Berman HM, Bhikadiya C, et al. RCSB Protein Data Bank: biological macromolecular structures enabling research and education in fundamental biology, biomedicine, biotechnology and energy. Nucleic Acids Res. 2019;47(D1):D464-d474.
19. Zhou C, Liu L, Zhuang J, et al. A Systems Biology-Based Approach to Uncovering Molecular Mechanisms Underlying Effects of Traditional Chinese Medicine Qingdai in Chronic Myelogenous Leukemia, Involving Integration of Network Pharmacology and Molecular Docking Technology. Med Sci Monit. 2018;24:4305–16.
20. Feng B, Fang YT, Xu RS. [Research progress in modern clinical application and mechanism of Guizhi decoction]. Zhongguo Zhong Yao Za Zhi. 2018;43(12):2442–7.
21. Wong HS, Chen N, Leong PK, Ko KM. β-Sitosterol enhances cellular glutathione redox cycling by reactive oxygen species generated from mitochondrial respiration: protection against oxidant injury in H9c2 cells and rat hearts. Phytother Res. 2014;28(7):999–1006.

22. Loizou S, Lekakis I, Chrousos GP, Moutsatsou P. Beta-sitosterol exhibits anti-inflammatory activity in human aortic endothelial cells. Mol Nutr Food Res. 2010;54(4):551–8.
23. Chan YM, Varady KA, Lin Y, et al. Plasma concentrations of plant sterols: physiology and relationship with coronary heart disease. Nutr Rev. 2006;64(9):385–402.
24. Liu Y, Gao L, Guo S, et al. Kaempferol Alleviates Angiotensin II-Induced Cardiac Dysfunction and Interstitial Fibrosis in Mice. Cell Physiol Biochem. 2017;43(6):2253–63.
25. Leeya Y, Mulvany MJ, Queiroz EF, Marston A, Hostettmann K, Jansakul C. Hypotensive activity of an n-butanol extract and their purified compounds from leaves of Phyllanthus acidus (L.) Skeels in rats. Eur J Pharmacol. 2010;649(1–3):301–13.
26. Cui S, Tang J, Wang S, Li L. Kaempferol protects lipopolysaccharide-induced inflammatory injury in human aortic endothelial cells (HAECs) by regulation of miR-203. Biomed Pharmacother. 2019;115:108888.
27. Patel RV, Mistry BM, Shinde SK, Syed R, Singh V, Shin HS. Therapeutic potential of quercetin as a cardiovascular agent. Eur J Med Chem. 2018;155:889–904.
28. Maaliki D, Shaito AA, Pintus G, El-Yazbi A, Eid AH. Flavonoids in hypertension: a brief review of the underlying mechanisms. Curr Opin Pharmacol. 2019;45:57–65.
29. Gomolak JR, Didion SP. A role for innate immunity in the development of hypertension. Med Hypotheses. 2014;83(6):640–3.
30. Morillas P, de Andrade H, Castillo J, et al. Inflammation and apoptosis in hypertension. Relevance of the extent of target organ damage. Rev Esp Cardiol (Engl Ed). 2012;65(9):819–25.
31. Senchenkova EY, Russell J, Yildirim A, Granger DN, Gavins FNE. Novel Role of T Cells and IL-6 (Interleukin-6) in Angiotensin II-Induced Microvascular Dysfunction. Hypertension. 2019;73(4):829–38.
32. Zhang X, Meng F, Song J, et al. Pentoxifylline Ameliorates Cardiac Fibrosis, Pathological Hypertrophy, and Cardiac Dysfunction in Angiotensin II-induced Hypertensive Rats. J Cardiovasc Pharmacol. 2016;67(1):76–85.
33. Liu D, Zeng X, Li X, Mehta JL, Wang X. Role of NLRP3 inflammasome in the pathogenesis of cardiovascular diseases. Basic Res Cardiol. 2018;113(1):5.
34. Ritter AMV, Faria APC, Sabbatini A, et al. MCP-1 Levels are Associated with Cardiac Remodeling but not with Resistant Hypertension. Arq Bras Cardiol. 2017;108(4):331–8.
35. Muñoz-Durango N, Fuentes CA, Castillo AE, et al. Role of the Renin-Angiotensin-Aldosterone System beyond Blood Pressure Regulation: Molecular and Cellular Mechanisms Involved in End-Organ Damage during Arterial Hypertension. Int J Mol Sci. 2016, 17(7).
36. Sakata Y, Yamamoto K, Mano T, et al. Activation of matrix metalloproteinases precedes left ventricular remodeling in hypertensive heart failure rats: its inhibition as a primary effect of Angiotensin-converting enzyme inhibitor. Circulation. 2004;109(17):2143–9.

37. Gkaliagkousi E, Doumas M, Gavriilaki E, et al. Elevated levels of MMP-9 in untreated patients with stage I essential hypertension. Clin Exp Hypertens. 2012;34(8):561–6.
38. Zhou GF, Jiang YH, Ma DF, et al. Xiao-Qing-Long Tang Prevents Cardiomyocyte Hypertrophy, Fibrosis, and the Development of Heart Failure with Preserved Ejection Faction in Rats by Modulating the Composition of the Gut Microbiota. Biomed Res Int. 2019, 2019:9637479.
39. Wang Y, Cui L, Xu H, et al. TRPV1 agonism inhibits endothelial cell inflammation via activation of eNOS/NO pathway. Atherosclerosis. 2017;260:13–9.
40. Davel AP, Wenceslau CF, Akamine EH, et al. Endothelial dysfunction in cardiovascular and endocrine-metabolic diseases: an update. Braz J Med Biol Res. 2011;44(9):920–32.
41. Mo L, Xu G, Wu C, et al. Key Regulatory Effect of Activated HIF-1α/VEGFA Signaling Pathway in Systemic Capillary Leak Syndrome Confirmed by Bioinformatics Analysis. J Comput Biol. 2020;27(6):914–22.
42. Jamwal S, Sharma S. Vascular endothelium dysfunction: a conservative target in metabolic disorders. Inflamm Res. 2018;67(5):391–405.
43. Tang DD, Niu HX, Peng FF, et al. Hypochlorite-Modified Albumin Upregulates ICAM-1 Expression via a MAPK-NF-κB Signaling Cascade: Protective Effects of Apocynin. Oxid Med Cell Longev. 2016, 2016:1852340.
44. Avendaño MS, Martínez-Revelles S, Aguado A, et al. Role of COX-2-derived PGE2 on vascular stiffness and function in hypertension. Br J Pharmacol. 2016;173(9):1541–55.
45. Hu F, Lou Y, Shi J, et al. Baseline serum albumin and its dynamic change is associated with type 2 diabetes risk: A large cohort study in China. Diabetes Metab Res Rev. 2020;36(5):e3296.
46. Van Hauwermeiren F, Vandenbroucke RE, Libert C. Treatment of TNF mediated diseases by selective inhibition of soluble TNF or TNFR1. Cytokine Growth Factor Rev. 2011;22(5–6):311–9.
47. Sanz-Rosa D, Oubiña MP, Cediel E, et al. Effect of AT1 receptor antagonism on vascular and circulating inflammatory mediators in SHR: role of NF-kappaB/IkappaB system. Am J Physiol Heart Circ Physiol. 2005;288(1):H111–5.
48. Familtseva A, Chaturvedi P, Kalani A, et al. Toll-like receptor 4 mutation suppresses hyperhomocysteinemia-induced hypertension. Am J Physiol Cell Physiol. 2016;311(4):C596-c606.
49. Zhang Z, Yao L, Yang J, Wang Z, Du G. PI3K/Akt and HIF–1 signaling pathway in hypoxia–ischemia (Review). Mol Med Rep. 2018;18(4):3547–54.
50. Shi L, Zhang G, Zheng Z, Lu B, Ji L. Andrographolide reduced VEGFA expression in hepatoma cancer cells by inactivating HIF-1α: The involvement of JNK and MTA1/HDCA. Chem Biol Interact. 2017;273:228–36.
51. Chen BC, Hung MY, Wang HF, et al. GABA tea attenuates cardiac apoptosis in spontaneously hypertensive rats (SHR) by enhancing PI3K/Akt-mediated survival pathway and suppressing Bax/Bak dependent apoptotic pathway. Environ Toxicol. 2018;33(7):789–97.

52. Lee JH, Parveen A, Do MH, Lim Y, Shim SH, Kim SY. Lespedeza cuneata protects the endothelial dysfunction via eNOS phosphorylation of PI3K/Akt signaling pathway in HUVECs. Phytomedicine. 2018;48:1–9.
53. Tanaka M. Improving obesity and blood pressure. Hypertens Res. 2020;43(2):79–89.
54. Mahat RK, Singh N, Arora M, Rathore V. Health risks and interventions in prediabetes: A review. Diabetes Metab Syndr. 2019;13(4):2803–11.

Figures

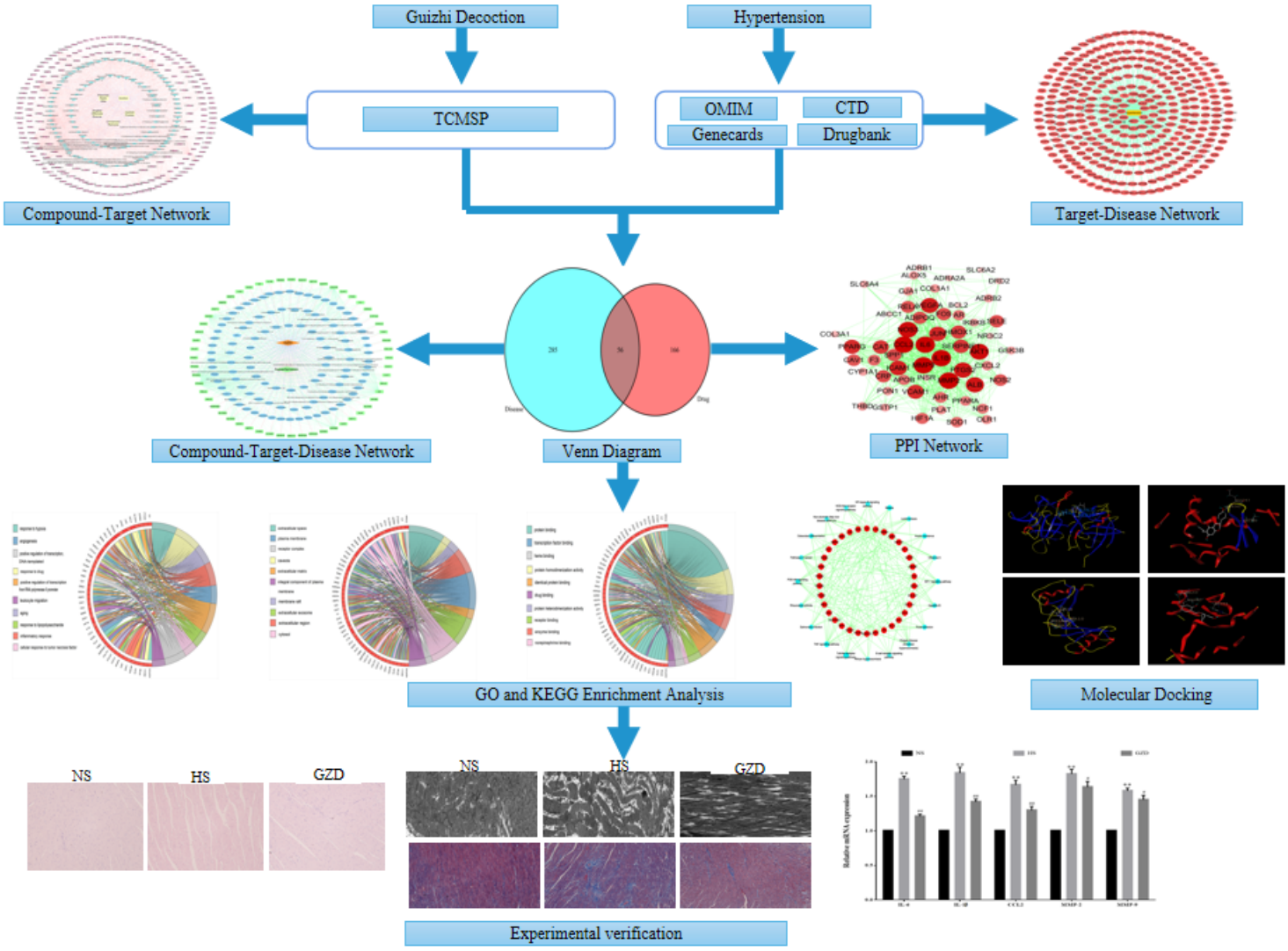

Figure 1

Study flowchart.

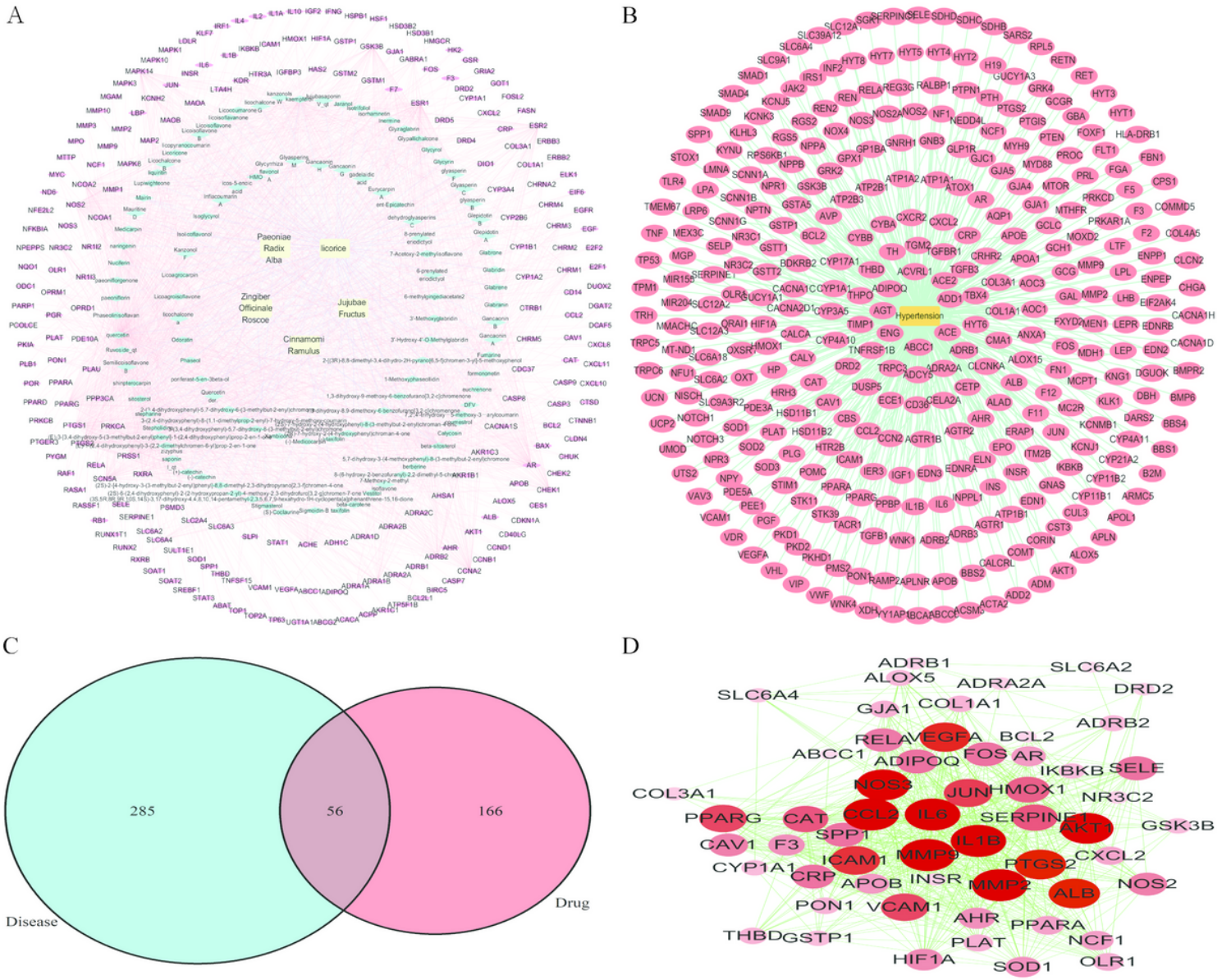

Figure 2

Guizhi decoction potential target-hypertension target network and analysis. a Compound-target (C-T) network of Guizhi decoction (GZD): The yellow node represents each herb of GZD, blue node represents the active compound, and purple node represents the target of the active compound; b Disease-target (D-T) network of hypertension: The red node represents the hypertension-related target; c The Venn diagram shows 56 overlapping targets between hypertension-related targets and active compound-related targets. (d) Protein-protein interaction (PPI) network of the 56 overlapping targets is shown here.

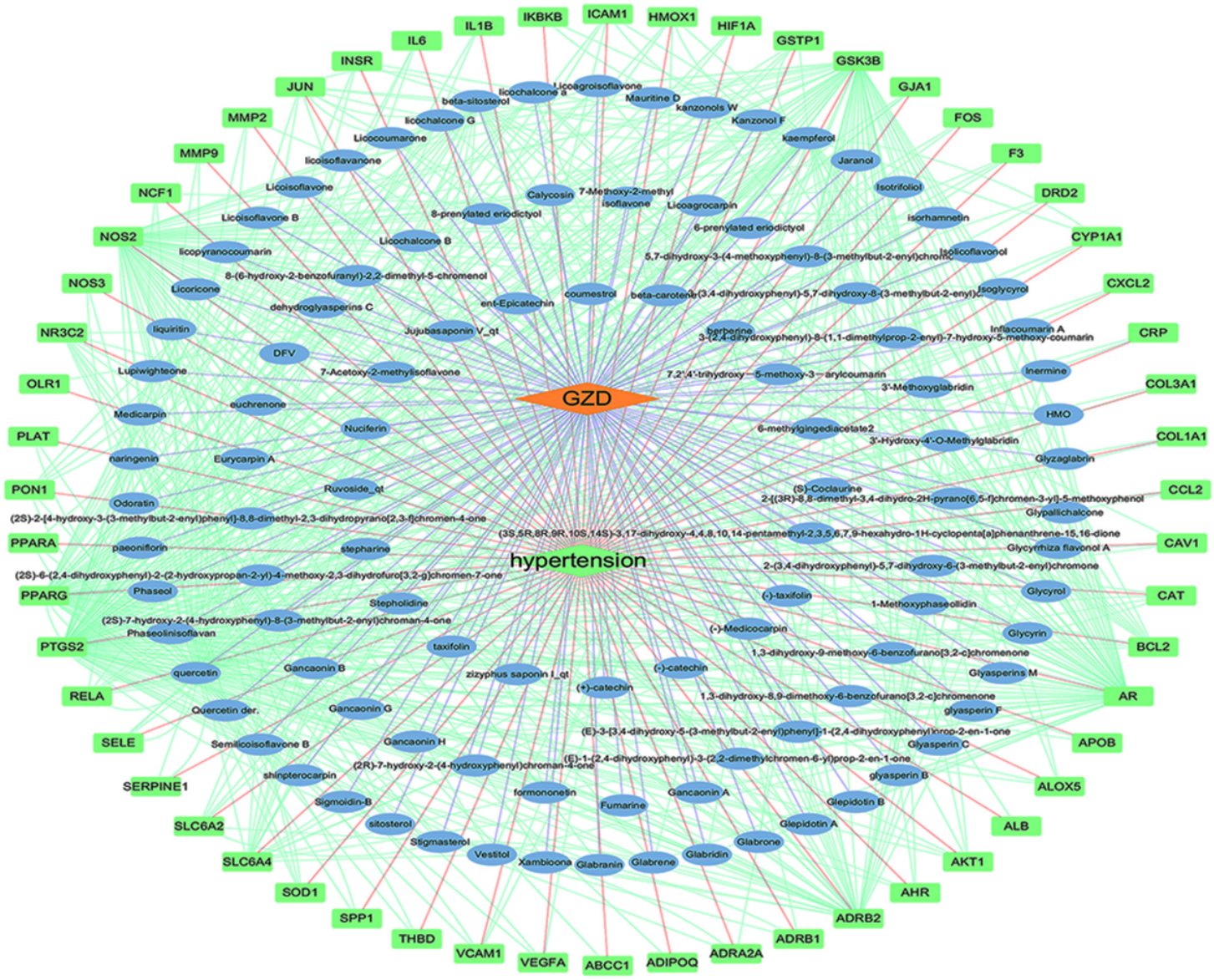

Figure 3

Compound-target-disease (C-T-D) network of Guizhi decoction (GZD) in the treatment of hypertension. The blue circle represents the active compound of GZD in the treatment of hypertension, and the green square pattern represents the overlapping targets.

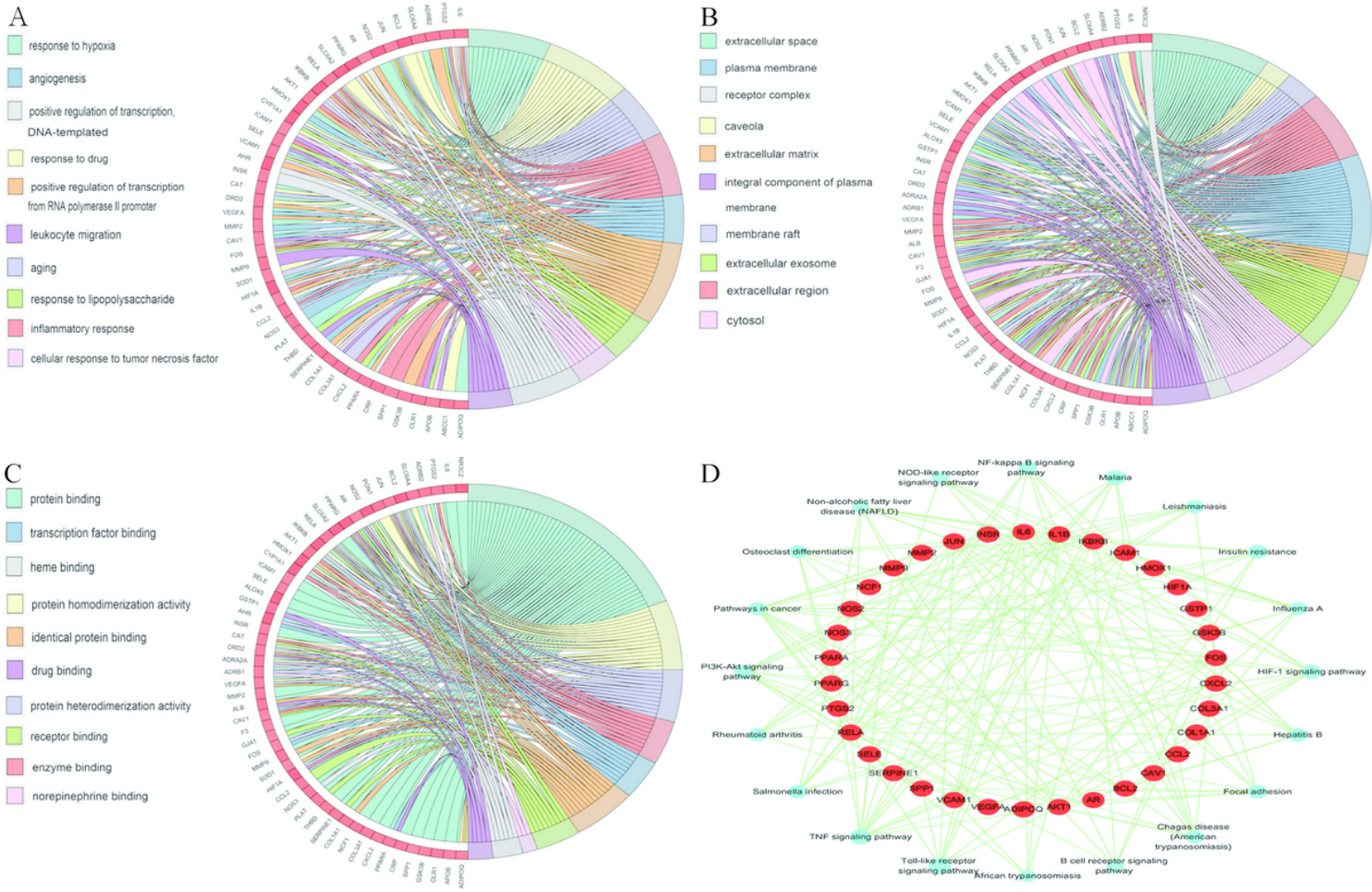

Figure 4

Results of gene ontology and Kyoto Encyclopedia of Genes and Genomes (KEGG) enrichment analysis. a The top 10 significantly enriched terms in biological process (BP); b The top 10 significantly enriched terms in cellular component (CC); c The top 10 significantly enriched terms in molecular function (MF); d Target-pathway network.

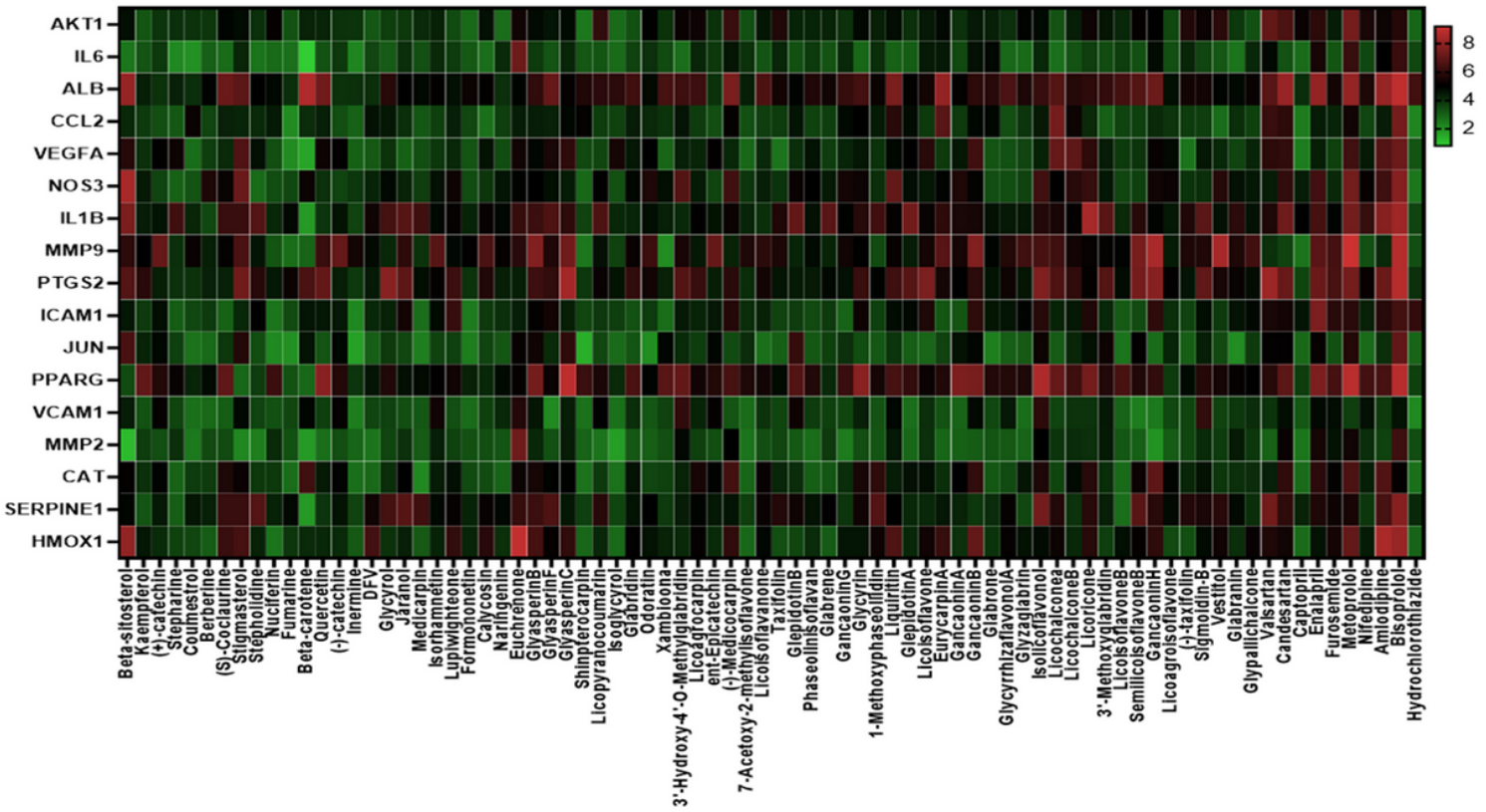

Figure 5

Heat maps of the docking scores of hub targets combining with active compounds in Guizhi decoction (GZD).

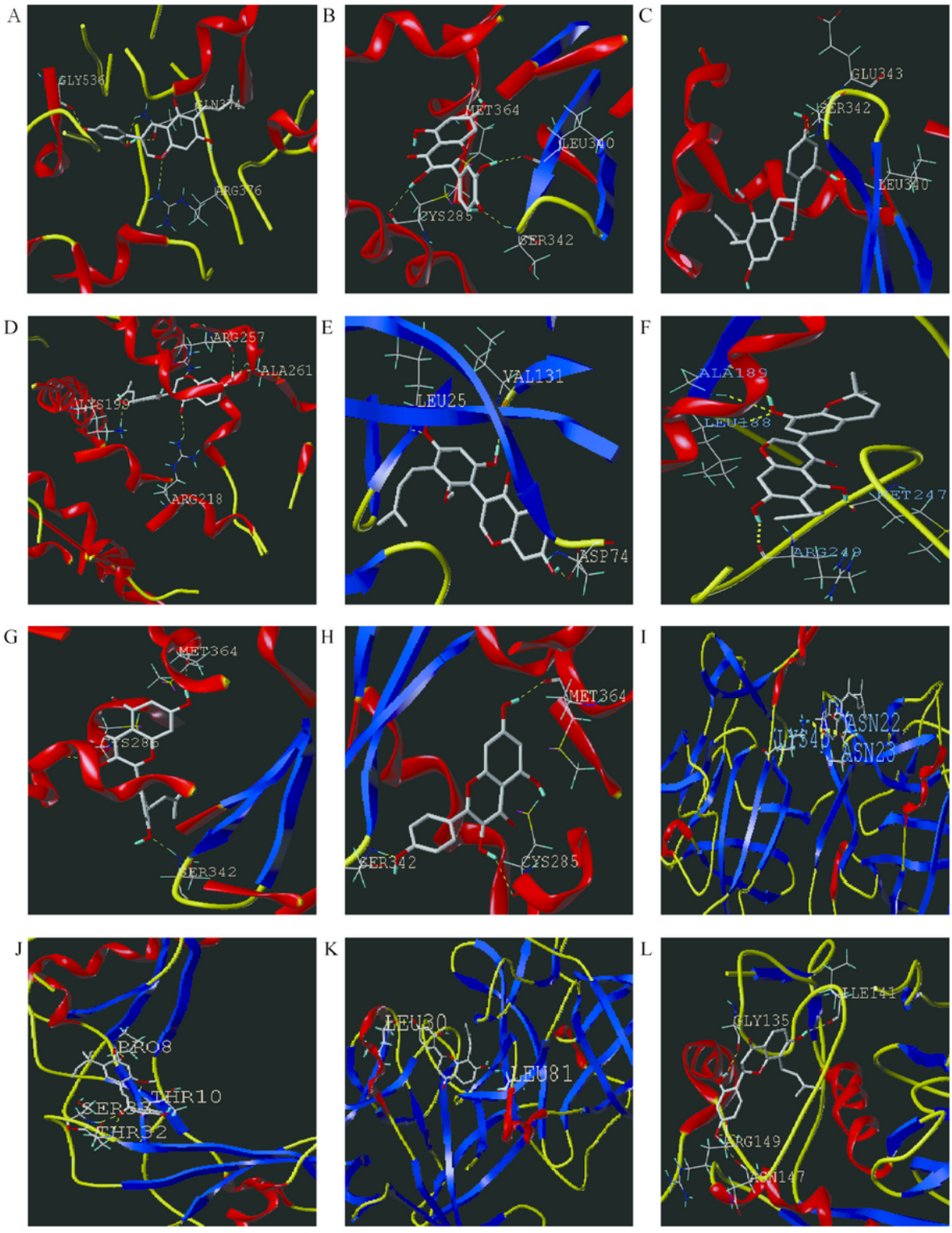

Figure 6

Action modes of active compounds with key targets. a Glyasperin C with PTGS2 (docking score = 8.33); b Quercetin with PPARG (docking score = 7.78); c Glyasperin C with PPARG (docking score = 8.86); d Eeurycarpin A with ALB (docking score = 8.02); e Licoricone with IL-1β (docking score = 8.44); f Gancaonin H with MMP-9 (docking score = 8.46); g Vestitol with MMP-9 (docking score = 8.42); h Kaempferol with PPARG (docking score =6.95); i β-sitosterol with IL-1β (docking score = 7.49); j

Licochalcone a with CCL2 (docking score = 7.38); k Euchrenone with IL-6 (docking score = 7.23); l Euchrenone with MMP-2 (docking score = 7.27).

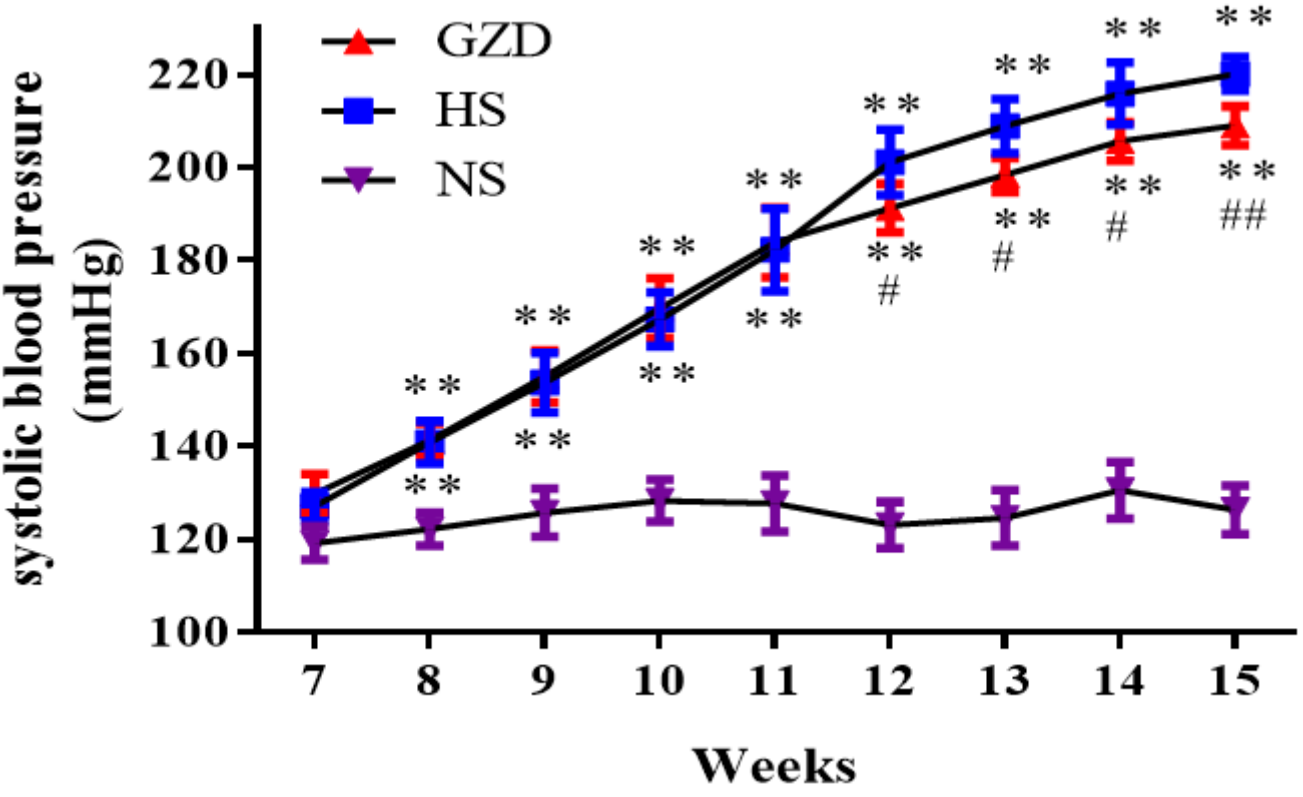

Figure 7

Guizhi decoction improved the level of blood pressure in Dahl salt-sensitive rats. All data are expressed as mean ± standard deviation (n = 8 rats per group). *p < 0.05, **p < 0.01 compared with the NS group; #p < 0.05, ##p < 0.01 compared with the HS group.

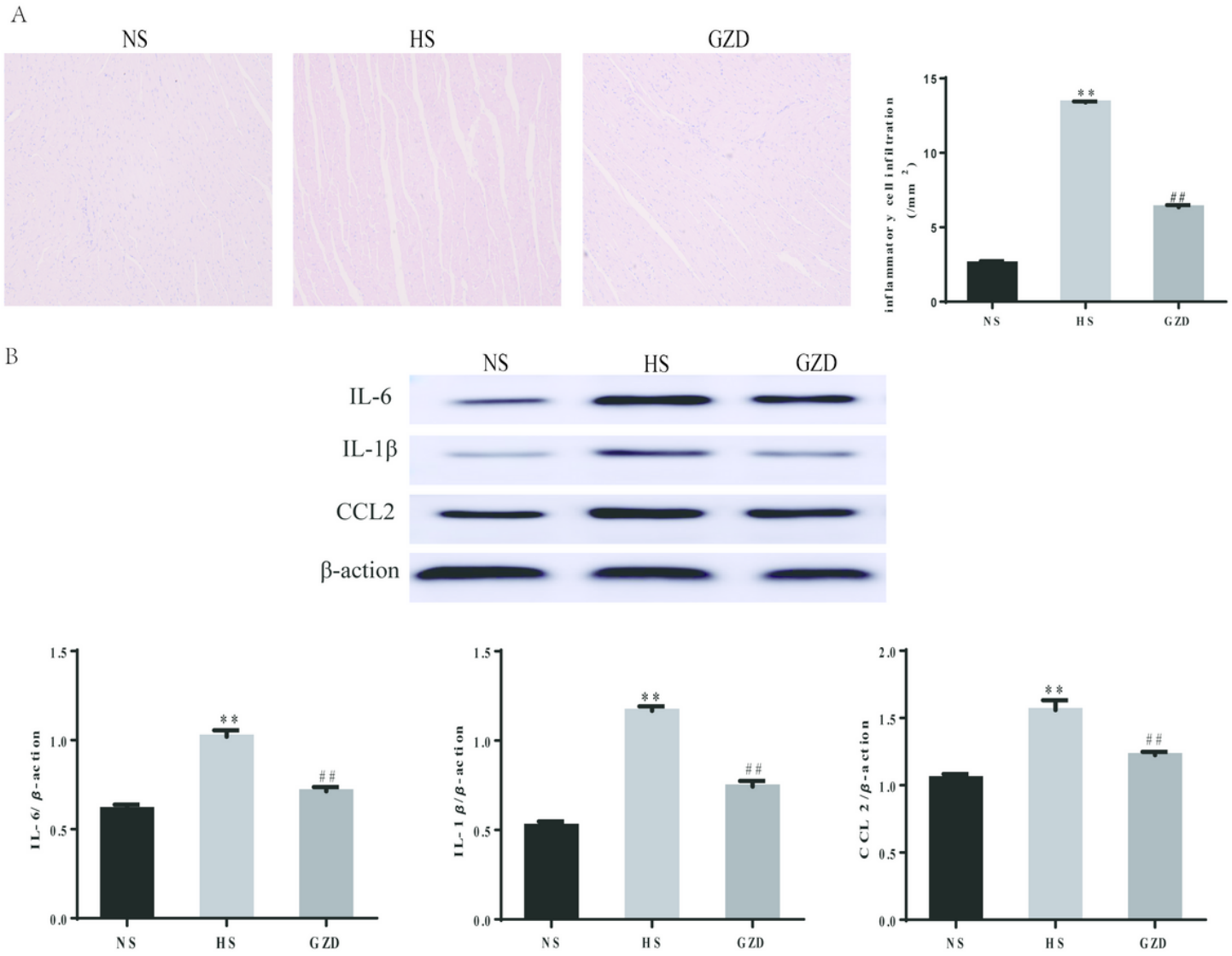

Figure 8

Guizhi decoction improved inflammation in Dahl salt-sensitive rats. a Histomorphological analysis of hematoxylin and eosin (H&E) stained sections (scale bars: 50 μm): Bar graphs show the degree of inflammatory cell infiltration; b The protein expressions of IL-6, CCL2, and IL-1β in the left ventricle are evaluated by western blot analysis. All data are expressed as mean ± standard deviation (n = 8 rats per group). *p < 0.05, **p < 0.01 compared with the NS group; #p < 0.05, ##p < 0.01 compared with the HS group.

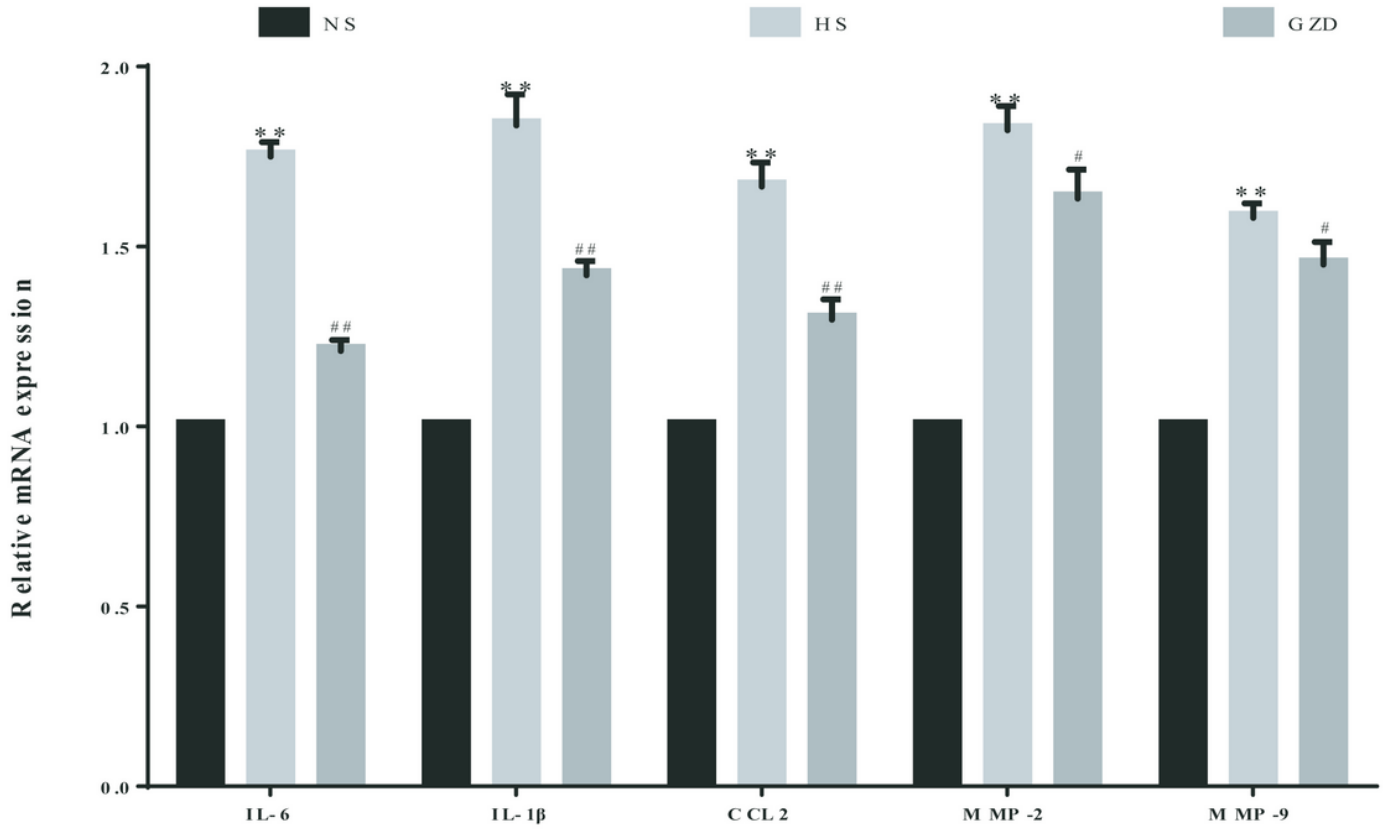

Figure 9

Guizhi decoction improved the relative mRNA expressions of IL-6, CCL2, IL-1β, MMP-2, and MMP-9 in Dahl salt-sensitive rats. All data are expressed as mean ± standard deviation (n = 8 rats per group). *p < 0.05, **p < 0.01 compared with the NS group; #p < 0.05 and ##p < 0.01 compared with the HS group.

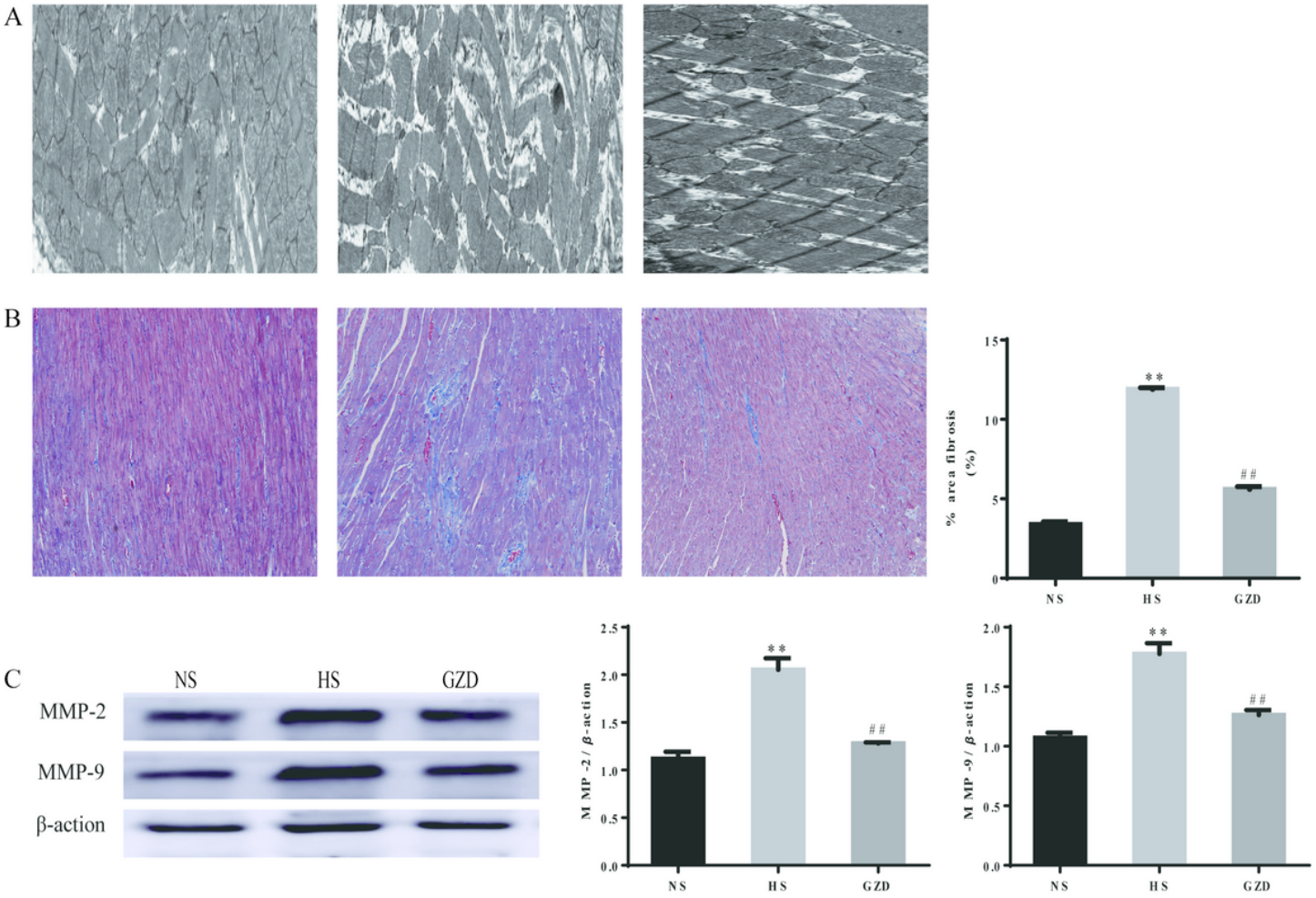

Figure 10

Guizhi decoction improved myocardial fibrosis in Dahl salt-sensitive rats. a Transmission electron microscopic images of the left ventricle (scale bars: 0.5 μm); b Histomorphological analysis of Masson staining: Bar graphs show the percentage of the fibrosed area of the left ventricle (scale bars: 50 μm); c The protein expressions of MMP2 and MMP9 in the left ventricle are evaluated by western blot analysis. All data are expressed as mean ± standard deviation (n = 8 rats per group). *p < 0.05, **p < 0.01 compared with the NS group; #p < 0.05 and ##p < 0.01 compared with the HS group.

Supplementary Files

This is a list of supplementary files associated with this preprint. Click to download.

- Additionalfile1TableS1.doc
- Additionalfile1TableS2.doc